Boreal Shield Forest Disturbance and Recovery Trends using Landsat Time Series

Ryan J. Frazier[1]*, Nicholas C. Coops[1], Michael A. Wulder[2]

Affiliations:

1) Department of Forest Resource Management, 2424 Main Mall, University of British Columbia, Vancouver, British Columbia, Canada V6T 1Z4

2) Canadian Forest Service (Pacific Forestry Center), Natural Resources Canada, Victoria, British Columbia, Canada, V8Z 1M5

(*) corresponding author.email: ryan.j.frazier@gmail.com

Key Words: Landsat; multitemporal; time series; boreal; forest, Boreal Shield; recovery; disturbance:

http://dx.doi.org/10.1016/j.rse.2015.09.015

Pre-print of published version

Reference: Frazier, R.J., N.C. Coops, and M.A. Wulder. (2015). Boreal Shield Forest Disturbance and Recovery Trends using Landsat Time Series. Remote Sensing of Environment. 170, 317-327.

DOI: http://dx.doi.org/10.1016/j.rse.2015.09.015

Highlights:

- We develop and apply a Landsat time series methodology for spectral recovery
- East & West Ca. Boreal Shield section's disturbance/recovery trends are compared
- Disturbance and recovery trends are different in each Boreal Shield sections
- Differences in recovery are apparent from spatial tabulation of recovery rates
- Selection of spectral index affects the characterization of recovery through time

Abstract:

Monitoring forest recovery following disturbance is important for both forest management as well as assessing possible climate change impacts on forest dynamics. To do so, an improved understanding of forest recovery processes and their relationship to remotely sensed spectral measures of recovery is required. Our objective in this research is to develop and apply a methodology for using Landsat time series to characterize forest recovery using spectral recovery trajectories. We focus our efforts in the Canadian Boreal Shield ecozone where a known geographic east to west distinction in disturbance regimes remains to be quantified. Results show that forest recovery following a stand replacing disturbance is detectable and quantifiable using a dense Landsat time series of spectral reflectance. All Tasseled Cap indices were found to capture an element of forest recovery following disturbance, with Wetness offering additional information on increasing vegetation structure and complexity. Tasseled Cap component trajectories of recovery show clear differences in both disturbance detection and forest recovery across the east and west Boreal Shield sections. The Cohen's d similarity metric indicated large differences ($d > .08$) in Wetness and Greenness-based spectral recovery trajectories when comparing the two Boreal Shield sections with the East Boreal Shield having markedly more above average recovery (+2 std. dev. from the mean) than the West. Based on our spectral recovery results, we also observe that forest recovery varies over the entire ecozone and is different between the east and west Boreal Shield forests

Introduction:

While variable based upon definitions, Canadian boreal forests represent about 30% of global boreal forests (Brandt et al. 2013, NRCan 2014). Wildfire is the primary disturbance agent in boreal forests, though insect infestation, windthrow, harvest, ice and snow related damage are all additional factors that can also occur with varying spatial pervasiveness and severity (Johnson 1996, Payette 1992, Brandt et al. 2013). Long-term averages indicate that wildfire occurs over approximately 2,000,000 hectares per year in Canada (Stocks et al 2002) with the most common being stand replacing crown and severe surface fires (Heinselman 1981). This fire regime has led to boreal tree species being well adapted to these fire disturbances, and often depending on fire to release the growing space from constraints imposed by the overstory (Oliver and Larson 1996, Brandt 2009, Bonan and Shugart 1989). As a consequence the boreal forest is a patchwork of forest structures, types, and ages, which is critical to maintaining the diversity and sustainability of the Canadian boreal zone (Bonan and Shugart 1989, Heinselman 1981).

The Canadian boreal can be stratified into ecozones which provide a spatial framework of ecologically homogenous units delineating distinct areas based on biophysical factors (Ecological Stratification Working Group 1996, Wiken 1986). The Boreal Shield ecozone is the largest unit stretching from Newfoundland into northern Saskatchewan with much of the area inaccessible and in a wilderness state. Despite the reported homogeneity of this ecozone, studies have suggested that the ecozone could be split along an east / west divide based on a number of distinct factors. Kurz et al (1992) suggested the ecozone be split due to differing ecoclimatic conditions. Kull et al (2006) split the ecozone citing colder and drier climes in the western section than the east. To characterize fire in the Canadian boreal forest, the ecozone was divided into eastern and western sections by Stocks et al (2002). Likewise, citing differing climatic patterns and forest processes, Andrew et al (2012) divided the Boreal Shield into two separate sections to aid their analysis of protected areas in Canada's boreal zone.

As a result of differing levels of accessibility (Andrew et al 2012), large areas of the Canadian Boreal Shield are not subject to direct anthropogenic influences with up to 35% and 40% of the forested East and West Boreal Shield ecozone sections not subject to any forest management practices (Shvidenko & Apps 2006, Wulder et al 2007). Thus the Boreal Shield can be further divided into two management zones: a generally southern managed portion that enjoys a relative wealth of descriptive data, and a generally northern unmanaged section that is less well characterized. The different management zones create a divide in forest information, which leaves a large part of the ecozone uncharacterized. The lack of spatially explicit forest information for more than a third of the ecozone is a problem when assessing both current and future climate change (Price et al 2013). Increased productivity in temperature limited predominantly eastern boreal areas (Boisvenue and Running 2006), and increased quantity and severity of wildfire disturbances in drier western boreal areas (Flannigan et al 2005) is expected, highlighting the need for disturbance mapping and monitoring of the subsequent return of vegetation.

Remote sensing technology has demonstrated the capacity to monitor large areas and can offer marked insights into how different regions are potentially changing, both in terms of pressures on disturbance regimes as well as the subsequent recovery (Powers et al, 2015, Beck and Goetz 2011, Berner et al 2011, Xu et al 2013, Pickell et al 2014). To date, emphasis has been placed on mapping forest disturbance using remote sensing technologies (Eidenshink et al 2007, Guindon et al 2014, Steyaert et al 1997). Although forest disturbances are well characterized by remote sensing (Wulder et al 2009, Potapov et al 2008, Kasischke et al 2011, Loboda et al 2012), explicit monitoring of post disturbance forest conditions for signals of recovery using a remotely sensed time series of imagery is a relatively recent phenomenon (Griffiths et al 2014, Kennedy et al 2012, Schroeder et al 2011, Chen et al 2011, Gitas et al 2012). Forest recovery has typically been defined as the reestablishment of forest biomass, or canopy structure, following disturbance (Oliver and Larson 1996), making it a process rather than a state, and therefore observable using time series of remote sensing data (Kennedy et al 2012, Hermosilla et al 2015, Huang et al 2010, Zhu et al 2012). It is increasingly understood that characterization of the spectral recovery as observed from remote sensing of a recently disturbed forest can aid in identifying and monitoring the progression of the stand towards successful reestablishment and maturation (Schroeder et al 2011). Interestingly, Frolking et al (2009) identified the need for remote sensing approaches to examine the characterization of forest recovery to provide forest managers with valuable information such as successional state (Shatford et al 2007) as well as informing on regional or temporally varying recovery trends.

Forest recovery has been monitored using image based time series using a variety of approaches. The most common, used with varying success, is to develop a time series of a given spectral index which is then related to biophysical parameters at a range of spatial scales. (Chu et al 2013). Griffiths et al (2014) assessed variability in forest recovery both spatially and temporally across political jurisdictions in the Carpathian by defining spectral recovery as a combination of pre-disturbance spectral index values and the spectral magnitude of the disturbance. Kennedy et al (2012) defined spectral recovery as a ratio of the magnitude of the disturbance event to spectral conditions five years post disturbance and illustrated recovery differences between public and privately owned lands in the Pacific Northwest of the United States. In the same study

Kennedy et al (2012) showed that drier areas experienced slower recovery as opposed more moist areas across management regimes, ownership, and political lines. Thus meaningful information about forest recovery across large areas can be derived from remote sensing imagery based time series, providing useful data and facilitating decisions about forest recovery by managers and researchers alike.

Landsat time series analysis offers an effective approach to monitor large forested areas (Hermosilla et al 2015, Huang et al 2010, Zhu et al 2012) like the Boreal Shield ecozone for disturbances and can enable characterization of the subsequent vegetative recovery (Kennedy et al 2010). In this research we compare and contrast spectral forest recovery trajectories following forest disturbance across the east and west sections of the Boreal Shield ecozone by developing and then applying a methodology using Landsat time series imagery. To meet this objective we examine stand replacing disturbances and the subsequent spectral signals of recovery by constructing spectral trajectories of recovery. These trajectories are then compared to nominally undisturbed forested signals, and the extent and recovery rate trends examined and compared across the ecozone.

Study Area:

The Boreal Shield Ecozone (Figure 1) is generally characterized by rolling and hilly topography with many small lakes, streams and rocky outcrops. A precipitation gradient exists with higher amounts (1000mm) in the coastal east and less (400mm) in the more continental west (Urquizo et al 2000, Ecological Stratification Working Group 1996). July average maximum temperatures are 13°C for both sections, however the east typically has less severe winters with January average minimum temperatures of -1°C compared to the west with -20°C (Urquizo et al 2000, Ecological Stratification Working Group 1996). The Boreal Shield ecozone is dominated by forests of black (*Picea mariana*) and white spruce (*Picea glauca*) with the more southerly portions having a wider mix of broadleaf treed vegetation such as white birch (*Betula papyrifera*), trembling aspen (*Populus tremuloides*) as well as an array of needle leaf species such as white (*Pinus strobus*), and red (*Pinus resinosa*) and jack pine (*Pinus banksiana*) (Ecological Stratification Working Group 1996). As discussed, fire and harvest are the primary agents of stand replacing forest disturbances (Bergeron et al 2004, Bergeron et al 2000), with fires occurring more often over larger areas in the west than the east (Stocks et al 2002). Less common are disturbances caused by insect infestations, wind and storm related damage, and disease (Urquizo et al 2000).For the purpose of this study we follow the division of the Boreal Shield ecozone established by Kull et al (2006), who cited the colder and drier climate in the west resulting in differing forest processes. As depicted in Figure 1 the ecozone can be divided by southern managed zone, where commercial forestry activities are present, and a northern largely unmanaged (non-commercial) zone.

Methods

Data

Landsat

The Landsat World Referencing System (WRS-2) acquisition grid (185 x 185km) was used to create a stratified random non overlapping sample of Landsat scene footprints within the Boreal Shield ecozone (Tucker et al 2000,Wulder et al 2001, Healey et al 2006, Kennedy et al 2010, Masek et al. 2013). Scenes were required to be at least 50% within the Boreal Shield ecozone, with portions outside of the ecozone clipped from further analysis. The Earth Observation for Sustainable Development of Forests (EOSD) land cover dataset was used to mask water bodies and to define areas of forest cover within the selected Landsat scenes (Wulder et al 2008). Deciduous, coniferous, and mixed forested type classes from the EOSD were collapsed into one category to create a binary forest layer, which was then used as a second filter to ensure that scenes were dominated by forest cover (> 80%). The scenes were further filtered by forest management zone, removing any scene that was not at least 50% within one management zone or another; if a scene covered both management zones, it was clipped to the portion within the largest management zone. Scenes were then randomly selected from the final candidate pool, while minimizing differences in total area as possible. Out of a possible 185 scenes covering the Boreal Shield ecozone, a total of 8 Landsat scenes were selected covering over 200,000 km^2 or 25 % of the ecozone's forested area (Table 1).

Image Processing

In summary, each Landsat scene was subject to radiometric correction, cloud masking, yearly compositing, and then temporal segmentation using the LandTrendr algorithm (Kennedy et al. 2012). Temporal trajectory metrics were then extracted from the temporal segmentation results and used to characterize recovery following stand replacing disturbances and compared between the east and west sections.

Image Selection, Preprocessing, and Compositing

Once selected, the imagery was extracted from the Landsat archive based on two criteria: (i) an acquisition date within the typical boreal zone growing season (which corresponds to Julian days 152-243 and the calendar months of June, July, and August); (ii) cloud cover < 75%. A total of 1220 scenes were selected from the archive. The distribution of imagery over the years for each scene is displayed in Figure 2. All imagery was ortho-rectified and converted to surface reflectance using the Landsat

Ecosystem Disturbance Adaptive Process (LEDAPS) (Masek et al 2006). A cloud mask was produced for each image using the Function of mask (Fmask) algorithm (Zhu and Woodcock 2012). Pixels delineated as cloud, cloud shadow, ice and snow were masked and not used in the remainder of the analysis.

An annual time series for each of the eight Landsat scenes was constructed from the multiple images per year using rules developed by Kennedy et al (2010): i) for each year a base image was selected based on its proximity to July 19th (Julian day 200), coinciding with the mid-growing season; ii) all other images in order of their proximity to July 19th within the same year were then used to fill in any areas that had been masked in the base image. This compositing process was repeated for each of the 29 years in the analysis period.

Spectral Indices and Recovery

Recent studies have highlighted differences in spectral recovery depending on the spectral index examined (Pickell et al 2015, Banskota et al 2014, Cuevas-Gonzalez et al 2009, Epting and Verblya 2005). Frequently used in Landsat time series studies the Tasseled Cap transformation is a linear transformation of Landsat's spectral bands into three orthogonal axes of Brightness, Greenness, and Wetness using published coefficients (Crist and Ciccone 1984). Previous studies have found that Tasseled Cap Brightness provides an indication of overall pixel albedo; Greenness provides an indication of vegetation photosynthetic condition; and Wetness is sensitive to changes in forest structure (Cohen et al 1995, Collins & Woodcock 1996, Franklin et al 2000, Franklin et al 2002, Skakun et al 2003, Healey et al 2006).

After a stand replacing disturbance, the Tasseled Cap Components will have differing recovery trajectories responding to different properties of forest stands as the recovery process progresses:

> Brightness relates to the general albedo (Crist and Ciccone 1984) of the land surface and values are typically high after a stand replacing disturbance and remain high due to the lack of absorption from vegetation cover and increased exposure of soil and non photsynthetic vegetation (Banskota et al 2014). Throughout forest stand recovery Brightness values will reduce with time due to increasing vegetation cover and subsequent increased absorption of visible and NIR wavelengths. This reduction in Brightness is typically observed as the stand reinitiates and growing space becomes increasingly occupied. As a result Brightness is uniquely suited to detect if a disturbed forest stand is recovering and if vegetation is re-establishing post disturbance.

Greenness contrasts the visible with the near and shortwave infrared wavelengths. The absorption of visible radiation by vegetation, and scattering driven by leaf by structure in the near infrared combine to produce high Greenness values as dense leafy forest canopies develop (Crist and Ciccone 1984). Low Greenness values are typically due to lack of photosynthetic vegetation, or vegetation that is under considerable stress. After a stand replacing disturbance, Greenness would be anticipated to increase quickly due to its sensitivity to green vegetation (Pickell et al 2015).

Wetness was named for its response to moisture content in vegetation and soils, and relies heavily upon the shortwave infrared bands. High values of Wetness indicate an abundance of moist plant matter, while lower values indicate reduced vegetation (Crist and Ciccone 1984). Changes in forest structure have been related to changes in Wetness (Cohen et al 1995, Cohen and Spies 1992, Hansen et al 2001), similar to the changes a forest stand undergoes during the recovery process. As a forest stand recovers, structure becomes more complex, creating a denser, moister, and multifaceted canopy with crown shadows, branching, all of which are reflected by increased Wetness values. Thus Wetness is well suited to observe forest recovery due to its ability to detect structural changes over time.

Throughout the recovery process forest stands undergo many physical changes, which can be observed using Landsat based Tasseled Cap time series. However, the capability to detect change is limited over time by the asymptotical nature of reflected radiation from a closed and dense forest canopy, as passive optical remote sensors can mostly detect changes on the topmost reflective surface.

Temporal Segmentation

The LandTrendr temporal segmentation algorithm was used to reduce year to year noise over the time series and segment the Wetness spectral values into distinct phases of disturbance, recovery, and no change (Kennedy et al 2010, Powell et al 2010, Frazier et al 2014). LandTrendr divides each pixel’s time series using an iterative linear fitting model, establishing breakpoints that define periods of no change, losses, and gains within a temporal trajectory. Temporal trajectory metrics were then calculated from the resultant temporal segments (Kennedy et al 2010, Frazier et al 2014, Pflugmacher et al 2012). To detect and isolate stand replacing disturbance events within the time series, we followed Kennedy et al (2012) and applied thresholds to the largest (>700 change magnitude) and most rapid (<3 years) changes in Wetness to identify severe and short duration fire and harvest stand replacing disturbances.

Once disturbance events were identified using the Wetness trajectory, recovery trajectories that follow a disturbance event were isolated and only selected for further study if they exhibited a positive slope from the disturbance event to the end of the time period, to ensure second disturbances did not occur. Using the year of disturbance, all recovery trajectories were then normalized by the year of the disturbance (see Schroeder et al. 2011). The mean and standard deviation of the three tasseled cap components was computed annually for all recovery trajectories in the east and west sections. For comparison, a stable, no change, forest mean threshold and standard deviation were also calculated from 18,652,249 no change pixels in the eastern section and 19,443,793 pixels in the western section.

Finally, each recovery pixel in each year was classified using the annual rate of recovery into one of five Wetness recovery classes: far above average recovery, above average recovery, average recovery, below average recovery, and far below average recovery. The far above average recovery represented values 2+ standard deviations above the section mean while above average values were between 1 - 2 standard deviations above the average. The average recovery category was bounded by the ± 1 standard deviation from the recovery mean. Below average recovery was bounded by 1-2 standard deviations below the average. Pixels experiencing recovery that was more than 2 standard deviations below the mean were classified as far below average recovery. The amount of area for each disturbance and recovery category was also calculated as a percent of the total forest area under observation.

Cohen's *d* statistic

Traditional statistical significance tests using very large sample sizes can be misleading, as any small difference would be significant at some level and often unimportant in terms of causation (Johnson 1999). We required a statistic that did not take into account our sample size and could determine meaningful levels of difference between our stable forest signals and recovery trajectory, and then between both East and West Boreal Shield recovery mean sets. The Cohen's *d* statistic (Cohen 1988) can indicate similarity or difference in datasets regardless of sample sizes. Cohen's *d* is a standardized statistic similar to z-scores, allowing the similarity or difference between two datasets to be compared. Although not often used in remote sensing applications, Cohen's *d* has been applied in the biological and ecological fields to determine likeness or difference between samples. Studies have shown Cohen's *d* ability to determine differences between datasets, when traditional significance testing may have shown less than optimal results (Nakagawa et al 2007, Cavin et al 2013, Wesner et al 2012).

To calculate a d value, the means of two separate groups are subtracted and then divided by the pooled standard deviation as shown in the equation:

$$d = \frac{\bar{x}_1 - \bar{x}_2}{\sigma_{pooled}}$$

where $\bar{x}_1$ and $\bar{x}_2$ are the means of two groups, and σ_{pooled} is the pooled standard deviation and d is a Cohen's d value. As described by Cohen (1988) and demonstrated in further studies (Cavin et al 2013, Nakagawa et al 2007), predefined difference thresholds set at d values of 0.2, 0.5, and 0.8 indicate small, moderate, or large differences between two datasets respectively. We utilized Cohen's d to compare recovery trends across the Boreal Shield ecozone and to establish the degree of difference between stable and recovering vegetation, and difference between recovering vegetation in each Boreal Shield section.

Results:

Wetness Recovery Trajectories and Cohen's *d* Values

After a stand replacing disturbance, Wetness has been shown to increase with time, and often corresponds to increases in forest structure(Schroeder et al 2010). A positive Wetness recovery trajectory occurs in both the eastern and western Boreal Shield sections (Figure 3a). The eastern Boreal Shield initial Wetness value post disturbance is far below the stable range of no change vegetation, but after 15 years of recovery Wetness values have increased to be within the stable range. Wetness values then continue to increase until the end of the Landsat record when they resemble the stable, no change vegetation mean. The western trajectory shows a similar trend, reaching the stable range by year 16, however not exceeding the stable mean during the analysis period.

The eastern and western Cohen's d Wetness recovery trajectories (Figure 3b) indicate that both sections are initially very different, but end the analysis period with relatively little or no difference from their stable means. The d statistic for the eastern trajectory (2.09) indicates a large difference from its stable mean. After 25 years however the d value recovers to indicate no difference. The western trajectory's initial d value of 1.3 also indicates a large difference from its stable mean, but again after 22 years the trajectory crosses into the zone of no change forest. The trajectory ends at a d value of 0.37 indicating that the differences in Wetness of recovering vegetation and stable vegetation is small.

When comparing the eastern and western trajectories to each other (Figure 3b) the Cohen's d trajectory has an initial value of 0.01 indicating no initial difference between the two trajectories immediately following disturbance. After 20 years the recovery trajectories are markedly different from each other, and the comparison *d* trajectory ends at a value of 0.90 indicative of a large difference between the two Boreal Shield sections.

A summary of the Wetness, Greenness, Brightness, and associated Cohen's *d* trajectories are shown in Figures 3b-6b and Table 2. Each trajectory's start, midpoint and end difference levels and *d* values are presented for the eastern and western recovery trajectories, as well as the comparison *d* trajectory.

Greenness Recovery Trajectories and Cohen's *d* Values

Like the wetness trajectories Greenness recovery is expected to increase as vegetation returns to the stand, and photosynthetic capability of the stand increases. Both East and West Boreal Shield Greenness trajectories conform to the expected positive trend following disturbance (Figure 4a). The eastern trajectory begins below the stable mean and within the stable range, but then quickly increases above the stable mean in the first 5 years. By year 19 recovery Greenness means are above the stable range, with the trajectory stable at that level until the end of the time series. The western Greenness trajectory has a very similar trend also starting below its stable range and increasing to higher than stable mean values after 20 years of recovery, but not exceeding the stable range by the end of the trajectory.

Cohen's *d* Greenness recovery trajectories (Figure 4b) show similar shapes for the eastern and western Boreal Shield, but have different *d* ranges indicating similar recovery rates but different relationships to their no change stable means. The eastern *d* trajectory's initial value of 0.49 indicates little difference from its stable mean, but after 5 years is not different and after 18 years is within the negative large difference range, where the trajectory ends with a *d* value of -1.04 indicating the recovery mean has exceeded the stable mean. The western *d* trajectory's initial *d* value of 0.90 indicates a large difference from its stable mean, decreasing by year 17 to be within the no difference zone, remaining there until the end of the time series with a *d* value of 0.03. This suggests that the Greenness signal from recovering vegetation is indistinguishable from stable mature forest vegetation after 18 years in the western Boreal Shield, however the eastern recovery trajectory shows more complicated trends.

The eastern and western Greenness Cohen's *d* comparison trajectory initial value of 0.50 indicates moderate difference (Figure 4b) between the two Greenness recovery trajectories. The *d* values quickly increase and by year 5 are within the large difference zone, remaining there until the end at a *d* value of 1.31. The high comparison *d* values

(>0.8) from 4 years post disturbance until the end of the comparison trajectory indicate that Greenness recovery is largely different between both Boreal Shield sections.

Brightness Recovery Trajectories and Cohen's *d* Values

As a stand recovers from a stand replacing disturbance Brightness will likely decrease representing an increase in canopy cover and a reduction in overall albedo. The eastern Brightness trajectory conforms to this expectation, however the western trajectory shows no trend (Figure 5a). The eastern trajectory starts above its stable range and ends above the stable mean. The western trajectory starts within the stable range and remains there throughout its entire trajectory finishing at similar initial Brightness values. Differences between the eastern and western trajectories are mirrored in their Cohen's *d* trajectories (Figure 5b). The eastern *d* trajectory's initial value of -0.84 indicates a large difference from the stable mean. The trajectory then crosses into the moderate difference zone after 13 years and ends within the little difference zone with a *d* value of -0.49. The western *d* trajectory's initial value of -0.36 is within the little difference zone and stays within that zone for the remainder of the analysis period with a final *d* value of -0.48.

The Brightness comparison Cohen's *d* trajectory decreases over time with an initial value of 0.51 within the moderate difference zone (Figure 5b). After 20 years the trajectory crosses into the little difference zone and ends with a *d* value of 0.21 near the lower bounds of the same zone signalling that recovering vegetation is always somewhat different between the two sections, however becoming more similar as time since disturbance time increases.

Areal Disturbance and Recovery Trends

The total yearly area disturbed in the eastern Boreal Shield sample shows a constant pattern of disturbances between 1985-2000 (Figure 6). Between 2001-2012 there is a marked increase in disturbed forest area. The western Boreal Shield shows a variable pattern of disturbance from 1985-2000 when compared to the eastern section, and again shows an increase in annual disturbance from 2001-2012.

The breakdown by trend rate for eastern and western Boreal Shield sections are shown in Figures 8 and 9 respectively as a percent of total forest area. A relatively stable disturbance trend in the eastern Boreal Shield from 1985 to 2000 is apparent from the yearly totals (Figure 7). The increasing annual percentage of disturbance is also evident from 2001-2012. The cumulative and classified recovery categories shown in Figure 7 demonstrates the variability in recovery rate after stand replacing disturbances. Most apparent is the marked relative increases in the areas that are classified as far above average recovery rate, defined as being 2 or more standard deviations above mean Wetness recovery.

Variable disturbance trends characterize the western Boreal Shield between 1985-2000 as is evident from the yearly totals (Figure 8). An increasing amount of disturbance from 2001-2012 is evident as well as an increase in the area undergoing far above average recovery, similar to the eastern section. Throughout the same period, the amount of area classified as having an average rate of recovery remains stable from 2001-2012, at a level of about 0.5% of total forested area of the Boreal Shield.

Discussion:

In this research we examined the utility of Landsat time series analysis to characterize disturbance and recovery trends across the boreal forests of the Canadian Boreal Shield ecozone. We discuss the results under two broad headings: temporal trajectory considerations and recovery characterization, and then our case study partitioning of the East and West Boreal Shield.

Temporal Trajectory Considerations & Recovery Characterization

Forest recovery refers to the reestablishment of key forest biophysical variables following a disturbance event, and is a process not a state (Frolking et al 2009). Forest recovery rates can differ due to severity, frequency and type of disturbance, site characteristics, and climate (Frolking et al 2009, Oliver and Larson 1996, Bolton et al 2015), Post disturbance forest recovery can take multiple pathways including (i) no recovery (e.g. land use conversion), (ii) recovery towards a predefined stocking or structure (e.g. plantation forestry), or (iii) natural recovery. Critical to any study of forest disturbance and recovery, regardless of location, is the rate that forest vegetation is returning from the disturbance event. However, the multiple ways in which forest recovery can be defined can lead to confusion when linking recovery to Landsat time series data. Chief among the concerns is that ecological and silvicultural definitions of forest recovery are not dependent on the actual presence of a mature forest, but more so predicated on provision of ecosystem services or emergent characteristics regarding treed vegetation height and canopy cover requirements.

Landsat time series can be used to characterize forest disturbance and forest recovery as shown in this work. The information generated from the Landsat time series aids in better understanding forest processes. Recovery extent, timing, and magnitude can now be reported and compared across large areas to inform on regional or temporally varying trends.

The terminology used by Oliver and Larson (1996) when describing forest stand dynamics is particularly useful when describing spectral forest recovery trajectories, as it grounds spectral forest recovery in easier to understand terms that are more generalizable and easier understood by a wider audience than spectral indices.

Oliver and Larson (1996) detail a generally applicable model of forest stand dynamics briefly summarized here with additional insight on how each Tasseled Cap component is affected. A stand replacing disturbance opens growing space for new individuals (Oliver and Larson 1996) causing an increase in albedo that in turn is reflected by increased in Brightness values. Individuals compete for resources until the canopy is closed, which causes large increases in Greenness and moderate increases in Wetness values, and a sharp decrease in Brightness. The stand reduces in density over time and the canopy increases in height (Oliver and Larson 1996) causing further increases in Wetness over time. An understory redevelops as growing space and resources are released by the canopy (Oliver and Larson 1996), which is mostly undetectable to each Tasseled Cap Index since it is occurring below the canopy. Shade tolerant individuals grow from the understory into the canopy supplanting dominant canopy species (Oliver and Larson 1996) potentially causing further change all three Tasseled Cap indices. The stand is then governed by gap dynamics caused by small disturbances (Oliver and Larson 1996 until a stand replacing disturbance occurs, which will restart the recovery process (Oliver and Larson 1996).

While the spectral recovery trajectories described above are simplified archetypes, the reality will be different as the combined elements that drive recovery (including initial disturbance severity, perception, and competition) can vary through a stands recovery, and thus effect the signals of recovery observed using Landsat time series. For example, the apparent linearity of our recovery trajectories is due to the selection for recovering stands that experience no further disturbances within our time series. In reality the recovery process will vary based upon the nature and amount of vegetation present over the course of forest recovery over time and could result in more complex and subtlety varied recovery trajectories. The within pixel averaging of the vegetation conditions will also serve to mute the year-on-year variability in spectral indices relating the vegetation recovery. Likwise, forest recovery monitoring using passive optical remote sensing are, by definition, limited to observing changes in reflected light from forest canopies. Previous efforts have demonstrated the difficulty inherent in assessing successional state from remote sensing datasets (Song et al 2007, Schroeder et al 2006, Song et al 2003). As a result, the spectral forest recovery trajectories do not necessarily directly correspond to changes in forest successional stages or may only be able to report on a small amount of variation in biophysical variables. Rather spectral trajectories essentially track the reestablishment of vegetation towards canopy closure or when the spectral signals of a recovering forest stand resemble that of nearby undisturbed vegetation or its previous state before the disturbance occurred (Kennedy et al 2012, Schroeder et al 2007, Buma 2012).

In this research we found that less than 1% of disturbed forests in both Boreal Shield sections showed no signs of recovery, with nearly all disturbed forests showing signs of recovery within 5 years. This implies that Boreal Shield forests overwhelmingly initiate recovery processes after stand replacing disturbances. This is in agreement with previous descriptions disturbance and subsequent recovery as key processes that shape the patchwork of forest structures, types, and ages critical to maintaining the diversity of the Canadian boreal zone (Bonan and Shugart 1989, Heinselman 1981). The spectral recovery trajectories constructed in this paper depend upon changes in Wetness through time. The shortwave infrared bands are weighted heavily in the calculation of Wetness when compared to the visible and near infrared bands (Crist et al 1984). As a result it is well suited to detecting changes from disturbance events such as fire. If a disturbance or recovery event produces an observable change in other portions of the spectrum other than the shortwave infrared, it is possible that this change may not be detected by the temporal segmentation algorithm. Thus care should be taken when selecting a spectral index and knowledge of the disturbance types of interest and their characteristics is useful. It is important to recall this link between the spectral channels used in a given index (or weight given in a combined index) with what is portrayed as recovery. An index will likely cross a non-disturbed forest threshold sooner with a visible and near-infrared driven index than an index driven by longer wavelengths. In this research, we have been conservative by focusing on the SWIR-driven Wetness index which has been shown to reflect changes in structural complexity and shadowing and is therefore more sensitive to the presence of trees, than early successional herbs and shrubs (Cohen et al 1995, Collins & Woodcock 1996, Franklin et al 2000). Alternatively, initial increases in vegetated cover are well characterized with shorter visible and near-infrared wavelengths (as used in Greenness). This more rapid saturation of the visible and near-infrared driven indices (i.e. Greenness) offers initial insight that vegetation is present but has less capacity for providing information on increasing structural complexity (Franklin et al 2000, Franklin et al 2002, Skakun et al 2003, Healey et al 2006).

Case Study: Partitioning of the East and West Boreal Shield

We were able to characterize forest recovery using Landsat time series, focusing our work on the known east/west division of the Boreal Shield ecozone. One of the rationales for splitting the Boreal Shield ecozone into two distinct features was that the regions experienced different ecoclimatic conditions, disturbance regimes, and forest processes. Using our temporally segmented datasets describing the disturbance and recovery trends in the both Boreal Shield sections, we suggest that characteristics of disturbance and recovery for the east and west Boreal Shield study areas are also different, further reinforcing the division of this ecozone.

The annual area disturbed shows different patterns of disturbance between the east and the west sections. From 1985-2000 there is a relatively constant area disturbed in the east. In contrast the west has a much more variable pattern of disturbance over the same time period (Figure 6). Interestingly, both the east and west show the same increasing disturbance trends in the 2001-2012 periods, but at differing amounts with more disturbances in the east than west.

The recovery trends of most eastern and western spectral indices follow the expected trend of an initial low value rising over time. However, Brightness trajectories are anticipated to begin with an initial high value and decrease over time. When the east and west Brightness section's trajectories are compared, large differences become apparent; the eastern trajectory follows a decreasing trend, while the western trajectory show no clear trend. We interpret this difference as related to the type and characteristics of disturbance that is most likely occurring. Bergeron et al (2004) demonstrated that fires are less frequent in the eastern than the western Boreal Shield and fire size is on average much larger in the west (Stocks et al 2002), which can lead to more patchiness and mixed severity effects. The clear decreasing pattern of Brightness in the east implies disturbances that are homogeneous entirely clearing a forest stand and leaving few if any remnant patches resulting in a uniform recovery signal. The lack of clear Brightness recovery trajectory in the west implies a more heterogeneous situation with mixed fire severities leaving more remnant patches that diminish the Brightness signal through the presence of more vegetation and decreased reflectivity in the visible wavelengths.

Spectral recovery trajectory patterns relative to their stable mean also highlight differences in the east and west sections. For example most eastern trajectories increase to their stable mean values (e.g. Wetness) and in some cases exceed their stable mean (e.g. Greenness). In contrast the western trajectories rarely exceed their stable mean, with most trajectories remaining below the mean throughout the analysis period (e.g. Wetness). We suggest these spectral recovery differences also relate known patterns of forest stand recovery between the two sections. After a stand replacing disturbance, eastern Boreal Shield forest stands have been shown to initiate with regenerating broad leaf shade intolerant treed vegetation, which have higher Wetness, and Greenness levels than the shade tolerant conifers that often replace as the stand matures (Bergeron et al 2000, Bergeron et al 2001, Bergeron et al 2007, Chen and Popadiouk 2002). After a stand replacing disturbance, western Boreal Shield stands typically initiate from the surviving seedbank and mature towards even aged shade tolerant conifers or more complex and layered conifer stands if another stand replacing disturbance does not occur (Bergeron et al 2000, Brassard and Chen 2006). This pattern is shown in the western Boreal Shield in the spectral recovery trajectory with lower Greenness, and Wetness values corresponding to the coniferous dominated re-initiating stand.

The classifications of recovery rates show differences between the east and west (Figures 8 and 9). While both areas show an increase in the above average recovery rate towards the end of their time series, this is more evident in the east than the west. Also the amount of average recovery in the western study areas remains relatively stable from year 14, the midpoint of our analysis period, until the end of the time series, while the eastern Boreal Shield study areas average recovery increases over the same period of time.

The Cohen's *d* statistic enabled the direct comparison of recovery patterns between the eastern and western Boreal Shield (Figures 3b-6b, Table 2). Three of four Cohen's *d* east to west comparison trajectories commence within zones of small or moderate difference and end with large difference between the two sections, indicating that their recovery is observably different. The difference between the east and west in Wetness recovery is especially important because it is sensitive to changes in forest structure. Noticeably, Wetness's comparison *d* trajectory shows the most change from its initial point of no difference (*d* value 0.01) ending with large differences (*d* value 0.90). This essentially means that although stand clearing disturbances may reduce the signal in disturbed areas in the east and west to similar Wetness levels, they recover from that level in different manners, as indicated by their Wetness recovery trajectories and their Cohen's *d* trajectories. Finally the comparison *d* trajectory shows that by the end of the time series, that east and west Boreal Shield recovery is largely ($d>0.8$) different.
It is important to recognize the factors that drive the variability in recovery between these two sections of the Boreal Shield ecozone. A known precipitation gradient exists, along with differences in winter average minimum temperatures, contributing to differing climates (Urquizo et al 2000, Ecological Stratification Working Group 1996) and as a result observed differences in vegetation recovery rates. Differences in disturbance frequency and size is already well known (Stocks et al 2002) for the two Boreal Shield sections which will also impact the observed spectral forest recovery. Additionally, soil conditions could also affect forest recovery rates (Lecomte and Bergeron 2005). The status and variability of all these factors combine to drive the observed differences in the east and west spectral forest recovery trajectories.

Conclusion:

The objective of this study was to develop and apply a methodology for using Landsat time series to characterize forest recovery using spectral recovery trajectories. To better understand spectral forest recovery, we selected and temporally segmented 1220 images from eight Landsat scenes to act as sample areas for the years 1984 through 2013 and then extracted signals of post-disturbance recovery. We constructed, characterized, and then compared spectral forest recovery trajectories in four spectral indices between both east and west Boreal Shield ecozone sections and examined difference levels in recovery with the Cohen's *d* statistic. We also directly compared the recovery trajectories of four spectral indices derived from the post disturbed areas within the east and west sections to each other showing similarities and differences.

Using yearly Landsat time series we characterized spectral recovery and further identified differences in recovery between the sections. We conclude that Landsat time series are an effective dataset to characterize disturbance and the subsequent recovery of forest vegetation. Spectral recovery is detectable, recovery trajectories are observable, and characterizations following a stand replacing disturbance provide insight into vegetative recovery and rates of recovery. Spatial trends of disturbance and recovery are evident and differ highlighting the differences between the two Boreal Shield sections. However, care must be taken when selecting a spectral index to temporally segment a time series as some indices capture early vegetation return and often saturate shortly thereafter. These indices therefore offer less information on post-disturbance vegetation return and related increases in vegetation complexity. Also important is the definition of recovery, as a process, and not necessarily a state. Further, the conditions that are sampled and used to indicate recovery must be clearly stated as the ability to achieve or resemble these conditions is a function of the strata that was created. In this particular research we created a strata of mature (stable, unchanged during the Landsat TM, ETM+, satellite record) forest conditions to compare to the spectral conditions present following stand replacing disturbances. All but 1% of the area disturbed had a positive spectral trajectory following disturbance, implying that 99% of the forest area disturbed is revegetating and initiating early successional processes leading towards a treed state.

Acknowledgements

We thank the USGS for open access to the Landsat imagery archive firstly, and secondly for making Landsat data available with a high level of preprocessing complete. Support for this research was provided by an NSERC Discovery to Coops and a UBC graduate scholarship to Frazier. Thanks are also given to three anonymous reviewers and the editors for their efforts and insightful and constructive comments.

References

Andrew, M. E., Wulder, M. A., & Coops, N. C. (2012). Identification of de facto protected areas in boreal Canada. Biological Conservation, 146, 97–10

Banskota, A., Kayastha, N., Falkowski, M. J., Wulder, M. A., Froese, R. E., & White, J. C. (2014). Forest monitoring using landsat time series data: a review. Canadian Journal of Remote Sensing, 40(5), 362-384.

Baumann, M., Ozdogan, M., Kuemmerle, T., Wendland, K. J., Esipova, E., & Radeloff, V. C. (2012). Using the Landsat record to detect forest-cover changes during and after the collapse of the Soviet Union in the temperate zone of European Russia. Remote Sensing of Environment, 124, 174-184.

Beck, P. S., & Goetz, S. J. (2011). Satellite observations of high northern latitude vegetation productivity changes between 1982 and 2008: ecological variability and regional differences. Environmental Research Letters, 6(4), 045501.

Bergeron, Y. (2000). Species and stand dynamics in the mixed woods of Quebec's southern boreal forest. Ecology, 81(6), 1500-1516.

Bergeron, Y., Drapeau, P., Gauthier, S., & Lecomte, N. (2007). Using knowledge of natural disturbances to support sustainable forest management in the northern Clay Belt. The Forestry Chronicle, 83(3), 326-337.

Bergeron, Y., Flannigan, M., Gauthier, S., Leduc, A., & Lefort, P. (2004). Past, current and future fire frequency in the Canadian boreal forest: implications for sustainable forest management. AMBIO: A Journal of the Human Environment,33(6), 356-360.

Bergeron, Y., Gauthier, S., Kafka, V., Lefort, P., & Lesieur, D. (2001). Natural fire frequency for the eastern Canadian boreal forest: consequences for sustainable forestry. Canadian Journal of Forest Research, 31(3), 384-391.

Berner, L. T., Beck, P. S., Bunn, A. G., Lloyd, A. H., & Goetz, S. J. (2011). High-latitude tree growth and satellite vegetation indices: Correlations and trends in Russia and Canada (1982–2008). Journal of Geophysical Research: Biogeosciences (2005–2012), 116(G1).

Boisvenue, C., & Running, S. W. (2006). Impacts of climate change on natural forest productivity–evidence since the middle of the 20th century. Global Change Biology, 12(5), 862-882.
Bolton, D. K., Coops, N. C., & Wulder, M. A. (2013). Measuring forest structure along productivity gradients in the Canadian boreal with small-footprint Lidar. Environmental Monitoring and Assessment, 185(8), 6617-6634.
Bonan, G. B., & Shugart, H. H. (1989). Environmental factors and ecological processes in boreal forests. Annual Review of Ecology and Systematics, 1-28.
Brandt, J. P., Flannigan, M. D., Maynard, D. G., Thompson, I. D., & Volney, W. J. A. (2013). An introduction to Canada's boreal zone: ecosystem processes, health, sustainability, and environmental issues 1. Environmental Reviews,21(4), 207-226
Brandt, J. P. (2009). The extent of the North American boreal zone. Environmental Reviews, 17, 101-161.
Brassard, B. W., & Chen, H. Y. (2006). Stand structural dynamics of North American boreal forests. Critical Reviews in Plant Sciences, 25(2), 115-137.
Buma, B. (2012). Evaluating the utility and seasonality of NDVI values for assessing post-disturbance recovery in a subalpine forest. Environmental Monitoring and Assessment, 184(6), 3849-3860.
Cavin, L., Mountford, E. P., Peterken, G. F., & Jump, A. S. (2013). Extreme drought alters competitive dominance within and between tree species in a mixed forest stand. Functional Ecology, 27(6), 1424-1435.
Chen, H. Y., & Popadiouk, R. V. (2002). Dynamics of North American boreal mixedwoods. Environmental Reviews, 10(3), 137-166.
Chen, X., Vogelmann, J. E., Rollins, M., Ohlen, D., Key, C. H., Yang, L., ... & Shi, H. (2011). Detecting post-fire burn severity and vegetation recovery using multitemporal remote sensing spectral indices and field-collected composite burn index data in a ponderosa pine forest. International Journal of Remote Sensing, 32(23), 7905-7927.
Chu, T., & Guo, X. (2013). Remote sensing techniques in monitoring post-fire effects and patterns of forest recovery in boreal forest regions: a review. Remote Sensing, 6(1), 470-520.
Cohen, J. (1988) Statistical power analysis for the behavioral sciences. 2nd Ed. Hove: Lawrence Erlbaum Associates.
Cohen, W. B., & Spies, T. A. (1992). Estimating structural attributes of Douglas-fir/western hemlock forest stands from Landsat and SPOT imagery. Remote Sensing of Environment, 41(1), 1-17.
Cohen, W. B., Fiorella, M., Gray, J., Helmer, E., & Anderson, K. (1998). An efficient and accurate method for mapping forest clearcuts in the Pacific Northwest using Landsat imagery. Photogrammetric Engineering and Remote Sensing, 64(4), 293-299.

Cohen, W. B., Spies, T. A., & Fiorella, M. (1995). Estimating the age and structure of forests in a multi-ownership landscape of western Oregon, USA. International Journal of Remote Sensing, 16(4), 721-746.

Collins, J. B., & Woodcock, C. E. (1996). An assessment of several linear change detection techniques for mapping forest mortality using multitemporal Landsat TM data. Remote Sensing of Environment, 56(1), 66–77.

Crist, E. P., & Cicone, R. C. (1984). A physically-based transformation of Thematic Mapper data---The TM Tasseled Cap. IEEE Transactions on Geoscience and Remote Sensing, IEEE Transactions On, (3), 256-263.

Cuevas-Gonzalez, M., Gerard, F., Balzter, H., & Riano, D. (2009). Analysing forest recovery after wildfire disturbance in boreal Siberia using remotely sensed vegetation indices. Global Change Biology, 15(3), 561-577.

Ecological Stratification Working Group. (1996). A national ecological framework for Canada. Agriculture and Agri-Food Canada and Environment Canada: Ottawa, ON. Available from: http://sis.agr.gc.ca/cansis/publications/ecostrat/cad_report.pdf [cited on May 12th 2015]

Eidenshink, J., Schwind, B., Brewer, K., Zhu, Z., Quayle, B., & Howard, S. (2007). A project for monitoring trends in burn severity. Fire Ecology 3 (1): 3-21.Fire Ecology Special Issue Vol, 3, 4.

Epting, J., Verbyla, D., & Sorbel, B. (2005). Evaluation of remotely sensed indices for assessing burn severity in interior Alaska using Landsat TM and ETM+. Remote Sensing of Environment, 96(3), 328-339.

Flannigan, M. D., Logan, K. A., Amiro, B. D., Skinner, W. R., & Stocks, B. J. (2005). Future area burned in Canada. Climatic Change, 72(1-2), 1-16

Franklin, S. E., Moskal, L. M., Lavigne, M. B., & Pugh, K. (2000). Interpretation and classification of partially harvested forest stands in the Fundy Model Forest using multitemporal Landsat TM. Canadian Journal of Remote Sensing, 26, 318−333.

Franklin, S.E., Lavigne, M.B., Wulder, M.A., & Stenhouse, G.B. (2002). Change detection and landscape structure mapping using remote sensing. The Forestry Chronicle. 78(5), 618-625

Frazier, R. J., Coops, N. C., Wulder, M. A., & Kennedy, R. (2014). Characterization of aboveground biomass in an unmanaged boreal forest using Landsat temporal segmentation metrics. ISPRS Journal of Photogrammetry and Remote Sensing, 92, 137-146.

Frolking, S., Palace, M. W., Clark, D. B., Chambers, J. Q., Shugart, H. H., & Hurtt, G. C. (2009). Forest disturbance and recovery: A general review in the context of spaceborne remote sensing of impacts on aboveground biomass and canopy structure. Journal of Geophysical Research: Biogeosciences (2005–2012), 114(G2).

Gitas, I., Polychronaki, A., Mitri, G., & Veraverbeke, S. (2012). Advances in remote sensing of post-fire vegetation recovery monitoring-a review. INTECH Open Access Publisher.

Goetz, S. J., Fiske, G. J., & Bunn, A. G. (2006). Using satellite time-series data sets to analyze fire disturbance and forest recovery across Canada. Remote Sensing of Environment, 101(3), 352-365.

Griffiths, P., Kuemmerle, T., Baumann, M., Radeloff, V. C., Abrudan, I. V., Lieskovsky, J., ... & Hostert, P. (2014). Forest disturbances, forest recovery, and changes in forest types across the Carpathian ecoregion from 1985 to 2010 based on Landsat image composites. Remote Sensing of Environment, 151, 72-88.

Guindon, L., Bernier, P. Y., Beaudoin, A., Pouliot, D., Villemaire, P., Hall, R. J., ... & St-Amant, R. (2014). Annual mapping of large forest disturbances across Canada's forests using 250 m MODIS imagery from 2000 to 2011.Canadian Journal of Forest Research, 44(12), 1545-1554.

Hansen, M. C., Potapov, P. V., Moore, R., Hancher, M., Turubanova, S. A., Tyukavina, A., ... & Townshend, J. R. G. (2013). High-resolution global maps of 21st-century forest cover change. Science, 342(6160), 850-853.

Hansen, M. J., Franklin, S. E., Woudsma, C., & Peterson, M. (2001). Forest structure classification in the North Columbia mountains using the Landsat TM Tasseled Cap Wetness component. Canadian Journal of Remote Sensing, 27(1), 20-32.

Healey, S. P., Cohen, W. B., Zhiqiang, Y., & Krankina, O. N. (2005). Comparison of Tasseled Cap-based Landsat data structures for use in forest disturbance detection. Remote Sensing of Environment, 97(3), 301-310.

Healey, S. P., Yang, Z., Cohen, W. B., & Pierce, D. J. (2006). Application of two regression-based methods to estimate the effects of partial harvest on forest structure using Landsat data. Remote Sensing of Environment, 101(1), 115-126.

Heinselman, M. L. (1981). Fire and succession in the conifer forests of northern North America. In Forest succession (pp. 374-405). Springer New York.

Hermosilla, T., Wulder, M. A., White, J. C., Coops, N. C., & Hobart, G. W. (2015). An integrated Landsat time series protocol for change detection and generation of annual gap-free surface reflectance composites. Remote Sensing of Environment, 158, 220-234

Huang, C., Goward, S. N., Masek, J. G., Thomas, N., Zhu, Z., & Vogelmann, J. E. (2010). An automated approach for reconstructing recent forest disturbance history using dense Landsat time series stacks. Remote Sensing of Environment, 114(1), 183-198.

Huang, C., Wylie, B., Yang, L., Homer, C., & Zylstra, G. (2002). Derivation of a Tasselled Cap transformation based on Landsat 7 at-satellite reflectance. International Journal of Remote Sensing, 23(8), 1741-1748.

Huete, A. R., Liu, H. Q., Batchily, K., & Van Leeuwen, W. J. D. A. (1997). A comparison of vegetation indices over a global set of TM images for EOS-MODIS. Remote Sensing of Environment, 59(3), 440-451.

Johnson, D. H. (1999). The insignificance of statistical significance testing. The Journal of Wildlife Management, 763-772.

Johnson, E. A. (1996). Fire and vegetation dynamics: studies from the North American boreal forest. Cambridge University Press.

Johnstone, J. F., & Chapin III, F. S. (2006a). Effects of soil burn severity on post-fire tree recruitment in boreal forest. Ecosystems, 9(1), 14-31.

Johnstone, J. F., & Chapin III, F. S. (2006b). Fire interval effects on successional trajectory in boreal forests of northwest Canada. Ecosystems, 9(2), 268-277.

Kasischke, E. S., & Turetsky, M. R. (2006). Recent changes in the fire regime across the North American boreal region—spatial and temporal patterns of burning across Canada and Alaska. Geophysical Research Letters, 33(9).

Kasischke, E. S., Loboda, T., Giglio, L., French, N. H., Hoy, E. E., de Jong, B., & Riano, D. (2011). Quantifying burned area for North American forests: Implications for direct reduction of carbon stocks. Journal of Geophysical Research: Biogeosciences (2005–2012), 116(G4).

Kennedy, R. E., Yang, Z., & Cohen, W. B. (2010). Detecting trends in forest disturbance and recovery using yearly Landsat time series: 1. LandTrendr—Temporal segmentation algorithms. Remote Sensing of Environment, 114(12), 2897-2910.

Kennedy, R. E., Yang, Z., Cohen, W. B., Pfaff, E., Braaten, J., & Nelson, P. (2012). Spatial and temporal patterns of forest disturbance and regrowth within the area of the Northwest Forest Plan. Remote Sensing of Environment, 122, 117-133.

Kull, S. J., Kurz, W. A., Rampley, G. J., Banfield, G. E., Schivatcheva, R. K., & Apps, M. J. (2006). Operational-scale carbon budget model of the Canadian forest sector (CBM-CFS3) version 1.0: user's guide. 2006.

Kurz, W.A.; Apps, M.J.; Webb, T.M.; McNamee, P.J. (1992). The carbon budget of the Canadian forest sector: Phase I. For. Can., Northwest Reg., Edmonton, AB. Inf. Rep. NOR-X-326

LeComte, N., Bergeron, Y. (2005). Successional pathways on different surficial deposits in the coniferous boreal forest of the Quebec Clay Belt. Canadian Journal of Forest Research, 2005, vol. 35, no 8, p. 1984-1995.

Lentile, L. B., Holden, Z. A., Smith, A. M., Falkowski, M. J., Hudak, A. T., Morgan, P., ... & Benson, N. C. (2006). Remote sensing techniques to assess active fire characteristics and post-fire effects. International Journal of Wildland Fire, 15(3), 319-345.

Loboda, T. V., Zhang, Z., O'Neal, K. J., Sun, G., Csiszar, I. A., Shugart, H. H., & Sherman, N. J. (2012). Reconstructing disturbance history using satellite-based assessment of the distribution of land cover in the Russian Far East. Remote Sensing of Environment, 118, 241-248.

Masek, J. G. (2001). Stability of boreal forest stands during recent climate change: evidence from Landsat satellite imagery. Journal of Biogeography, 28(8), 967-976.

Masek, J. G., Goward, S. N., Kennedy, R. E., Cohen, W. B., Moisen, G. G., Schleeweis, K., & Huang, C. (2013). United States forest disturbance trends observed using Landsat time series. Ecosystems, 16(6), 1087-1104.

Masek, J.G., E.F. Vermote, N. Saleous, R. Wolfe, F.G. Hall, Huemmrich, K.F., Gao, J. Kutler, and T.K. Lim, (2006), A Landsat surface reflectance data set for North America, 1990-2000, Geoscience and Remote Sensing Letters, 3, 68-72.

Mehrabi, Z., Slade, E. M., Solis, A., & Mann, D. J. (2014). The importance of microhabitat for biodiversity sampling. PloS one, 9(12), e114015.

Nakagawa, S., & Cuthill, I. C. (2007). Effect size, confidence interval and statistical significance: a practical guide for biologists. Biological Reviews,82(4), 591-605.

Natural Resources Canada. (2014). Boreal forest. Available from: https://www.nrcan.gc.ca/forests/boreal/13071. [Cited on May 12 2015].

Oliver, C. D., & Larson, B. C. (1990). Forest stand dynamics. McGraw-Hill, Inc..

Payette, S. (1992). Fire as a controlling process in the North American boreal forest. A systems analysis of the global boreal forest, 144-169.

Pflugmacher, D., Cohen, W.B., & Kennedy, R.E. (2012). Using Landsat derived disturbance history (1972-2012) to predict current forest structure. Remote Sensing of Environment, 122, 146-165.

Pickell, P.D., Hermosilla, T, Frazier, R.J., Coops, N.C., Wulder, M.A.. (2015). Forest recovery trends derived from Landsat time series for North American boreal forests. IN PREP.

Potapov, P. V., Turubanova, S. A., Tyukavina, A., Krylov, A. M., McCarty, J. L., Radeloff, V. C., & Hansen, M. C. (2014). Eastern Europe's forest cover dynamics from 1985 to 2012 quantified from the full Landsat archive. Remote Sensing of Environment.

Potapov, P., Hansen, M. C., Stehman, S. V., Loveland, T. R., & Pittman, K. (2008). Combining MODIS and Landsat imagery to estimate and map boreal forest cover loss. Remote Sensing of Environment, 112(9), 3708-3719.

Powell, S. L., Cohen, W. B., Healey, S. P., Kennedy, R. E., Moisen, G. G., Pierce, K. B., & Ohmann, J. L. (2010). Quantification of live aboveground forest biomass dynamics with Landsat time series and field inventory data: A comparison of empirical modeling approaches. Remote Sensing of Environment, 114, 1053–1068.

Powers, R. P., Hermosilla, T., Coops, N. C., & Chen, G. (2015). Remote sensing and object-based techniques for mapping fine-scale industrial disturbances. International Journal of Applied Earth Observation and Geoinformation, 34, 51-57.

Price, D. T., Alfaro, R. I., Brown, K. J., Flannigan, M. D., Fleming, R. A., Hogg, E. H., ... & Venier, L. A. (2013). Anticipating the consequences of climate change for Canada's boreal forest ecosystems 1. Environmental Reviews,21(4), 322-365.
Sader, S. A., Waide, R. B., Lawrence, W. T., & Joyce, A. T. (1989). Tropical forest biomass and successional age class relationships to a vegetation index derived from Landsat TM data. Remote Sensing of Environment, 28, 143-198.
Schroeder, T. A., Cohen, W. B., & Yang, Z. (2007). Patterns of forest regrowth following clearcutting in western Oregon as determined from a Landsat time-series. Forest Ecology and Management, 243(2), 259-273.
Schroeder, T. A., Cohen, W. B., Song, C., Canty, M. J., & Yang, Z. (2006). Radiometric correction of multi-temporal Landsat data for characterization of early successional forest patterns in western Oregon. Remote Sensing of Environment, 103(1), 16-26.
Schroeder, T. A., Wulder, M. A., Healey, S. P., & Moisen, G. G. (2011). Mapping wildfire and clearcut harvest disturbances in boreal forests with Landsat time series data. Remote Sensing of Environment, 115(6), 1421-1433.
Shatford, J. P. A., Hibbs, D. E., & Puettmann, K. J. (2007). Conifer regeneration after forest fire in the Klamath-Siskiyous: How much, how soon?. Journal of Forestry, 105(3), 139-146.
Shvidenko, A., & Apps, M. (2006). The International Boreal Forest Research Association: understanding boreal forests and forestry in a changing world. Mitigation and Adaptation Strategies for Global Change, 11(1), 5-32.
Skakun, R. S., Wulder, M. A., & Franklin, S. E. (2003). Sensitivity of the Thematic Mapper enhanced wetness difference index to detect mountain pine beetle red-attack damage. Remote Sensing of Environment, 86(4), 433–443.
Song, C., & Woodcock, C. E. (2003). Monitoring forest succession with multitemporal Landsat images: factors of uncertainty. IEEE Transactions on Geoscience and Remote Sensing, 41(11), 2557-2567.
Song, C., Schroeder, T. A., & Cohen, W. B. (2007). Predicting temperate conifer forest successional stage distributions with multitemporal Landsat Thematic Mapper imagery. Remote Sensing of Environment, 106(2), 228-237.
Steyaert, L. T., Hall, F. G., & Loveland, T. R. (1997). Land cover mapping, fire regeneration, and scaling studies in the Canadian boreal forest with 1 km AVHRR and Landsat TM data. Journal of Geophysical Research: Atmospheres (1984–2012), 102(D24), 29581-29598.
Stocks, B. J., Mason, J. A., Todd, J. B., Bosch, E. M., Wotton, B. M., Amiro, B. D., ... & Skinner, W. R. (2002). Large forest fires in Canada, 1959–1997. Journal of Geophysical Research: Atmospheres (1984–2012), 107(D1), FFR-5.
Urquizo, N., Bastedo, J., Brydges, T., & Shear, H. (2000). Ecological assessment of the boreal shield ecozone. Environment Canada, Ottawa, Ont. ISBN-662-28679-0.

Wesner, J. S., Billman, E. J., & Belk, M. C. (2012). Multiple predators indirectly alter community assembly across ecological boundaries. Ecology, 93(7), 1674-1682.

Wiken, E.B. (1986). Terrestrial ecozones of Canada. Ecological Land Classification Series No. 19. Environment Canada, Hull, Quebec.

Woodcock, C. E., Allen, R., Anderson, M., Belward, A., Bindschadler, R., Cohen, W., ... & Wynne, R. (2008). Free access to Landsat imagery. Science (New York, NY), 320(5879), 1011.

Wulder, M. A., Masek, J. G., Cohen, W. B., Loveland, T. R., & Woodcock, C. E. (2012). Opening the archive: How free data has enabled the science and monitoring promise of Landsat. Remote Sensing of Environment, 122, 2-10.

Wulder, M. A., Ortlepp, S. M., White, J. C., & Maxwell, S. (2008). Evaluation of Landsat-7 SLC-off image products for forest change detection. Canadian Journal of Remote Sensing, 34(2), 93-99.

Wulder, M. A., White, J. C., Alvarez, F., Han, T., Rogan, J., & Hawkes, B. (2009). Characterizing boreal forest wildfire with multi-temporal Landsat and LIDAR data. Remote Sensing of Environment, 113(7), 1540-1555.

Wulder, M. A., & Seemann, D. (2001). Spatially partitioning Canada with the Landsat worldwide referencing system. Canadian Journal of Remote Sensing, 27(3), 225-231.

Wulder, M.A., Campbell, C., White, J.C., Flannigan, M., & Campbell, I.D. (2007). National circumstances in the international circumboreal community. The Forestry Chronicle. 83(4), 539-556.

Xu, L., Myneni, R. B., Chapin Iii, F. S., Callaghan, T. V., Pinzon, J. E., Tucker, C. J., ... & Stroeve, J. C. (2013). Temperature and vegetation seasonality diminishment over northern lands. Nature Climate Change, 3(6), 581-586.

Zhang, Q., Pavlic, G., Chen, W., Latifovic, R., Fraser, R., & Cihlar, J. (2004). Deriving stand age distribution in boreal forests using SPOT Vegetation and NOAA AVHRR imagery. Remote Sensing of Environment, 91(3), 405-418.

Zhu, Z., & Woodcock, C. E. (2012). Object-based cloud and cloud shadow detection in Landsat imagery. Remote Sensing of Environment, 118, 83-94.

Zhu, Z., Woodcock, C. E., & Olofsson, P. (2012). Continuous monitoring of forest disturbance using all available Landsat imagery. Remote Sensing of Environment, 122, 75-91.

Figures

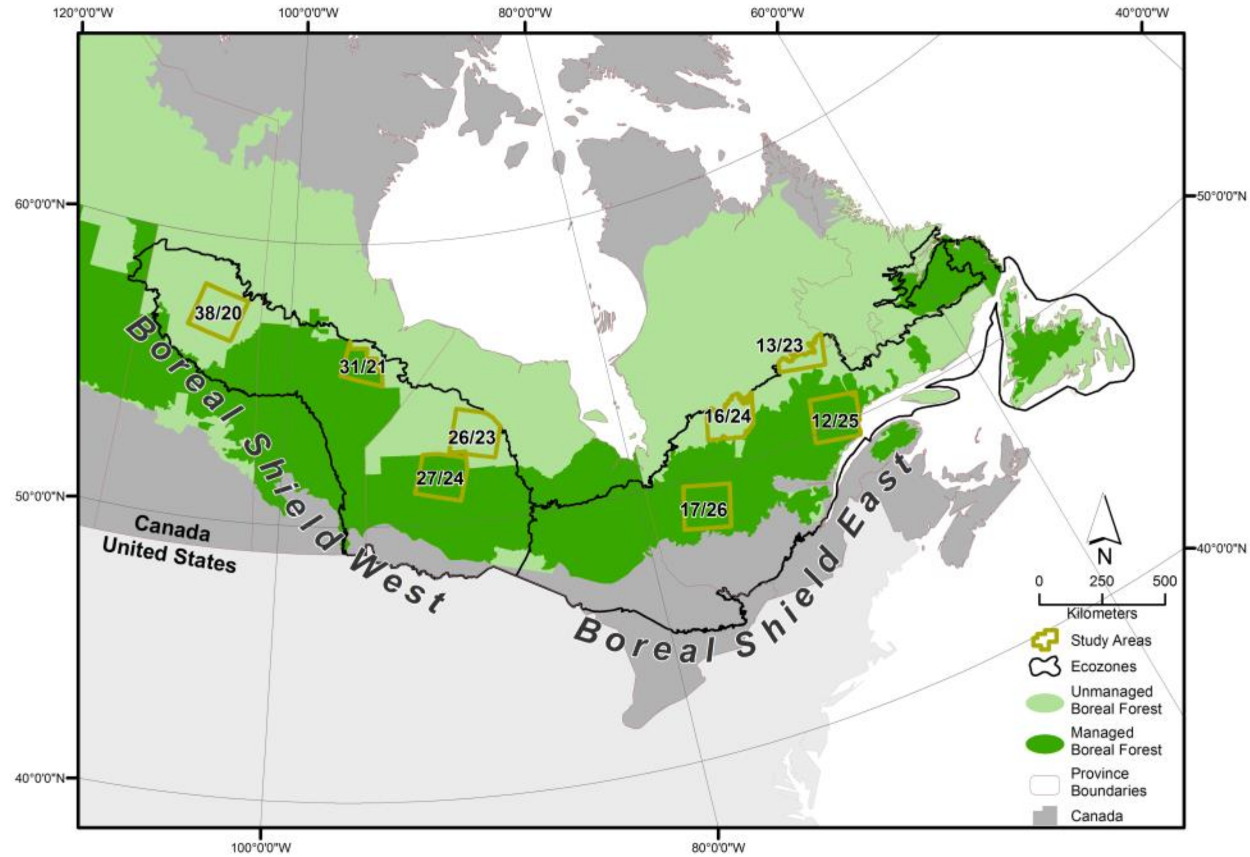

Figure 1: Boreal Shield East and West ecozones and forest management zones in Canada with the eight study scene portions shown.

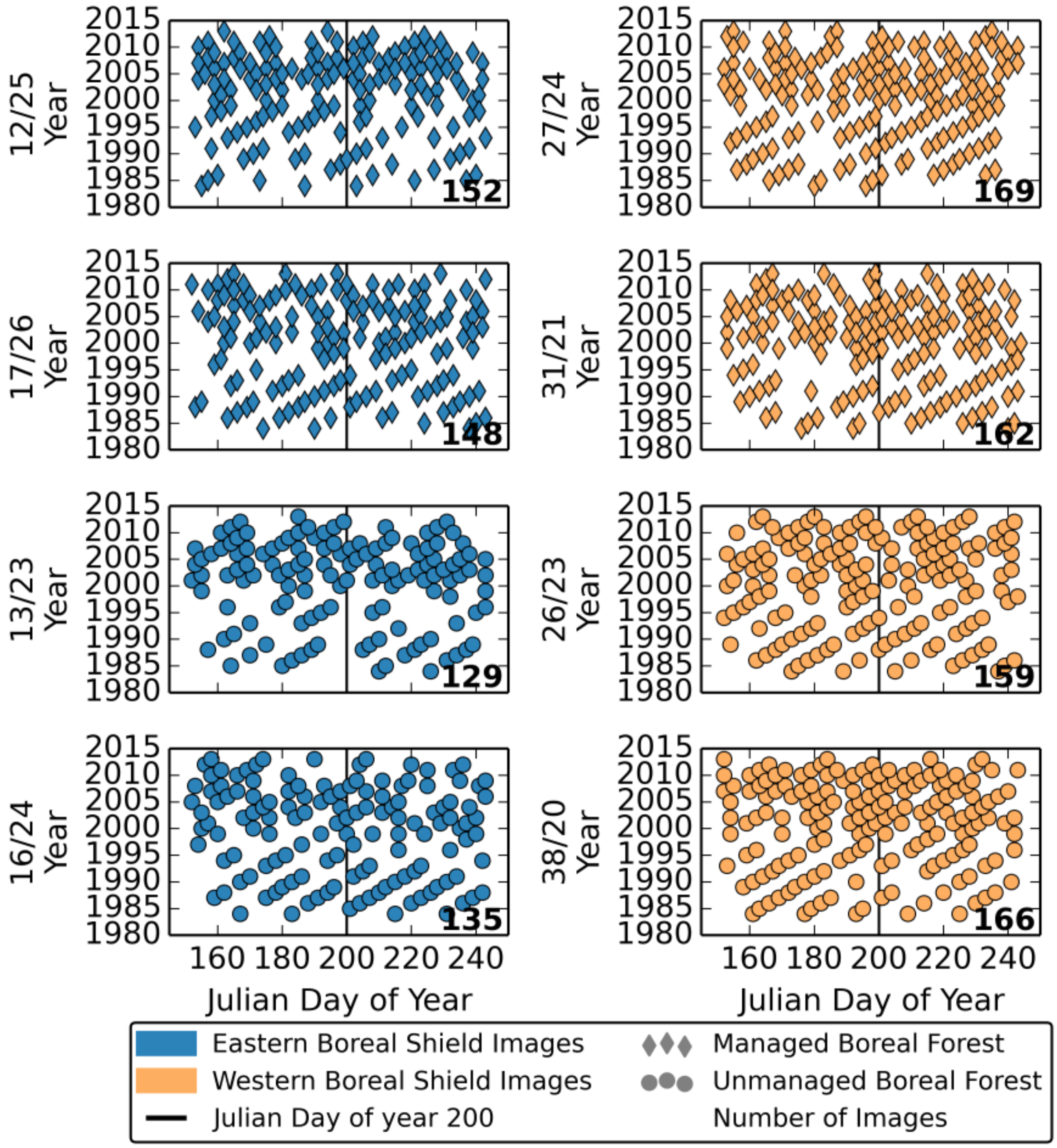

Figure 2: Distribution of dates and years of imagery for each Landsat footprint portion used in this study. Eastern Boreal Shield path row scene footprints are shown in blue while western Boreal Shield path row scene footprints are shown in orange. Diamond shaped symbols indicate images located in the management zone, while circle shaped symbols indicate images within the non-management zone. A total of 1220 images were used divided between the 8 scene footprints.

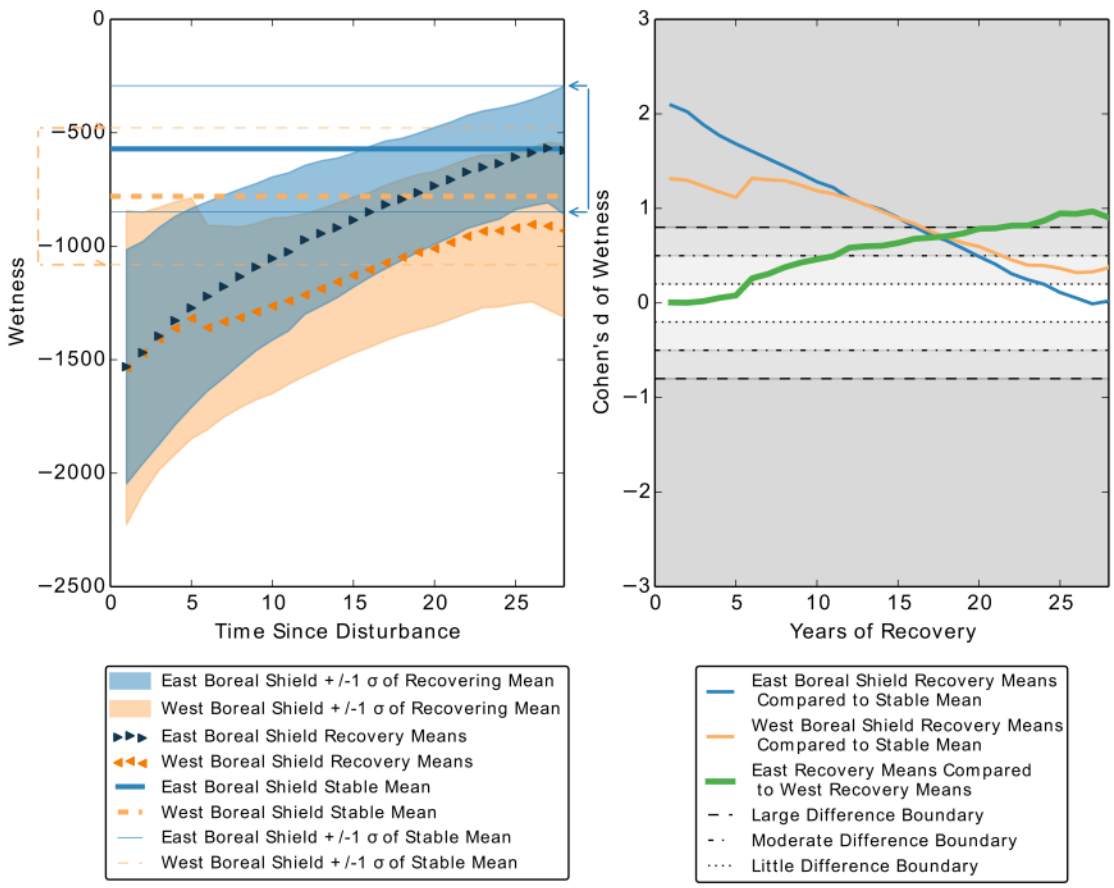

Figure 3: a) Observed Wetness recovery trajectory of each Boreal Shield section. Shading for each section shows +/-1 standard deviation of the recovery means per a year. Straight horizontal lines indicate the stable means and +/-1 standard deviation range for each Boreal Shield section. **b)** Cohen's *d* Wetness recovery trajectories for each Boreal Shield are shown with the predetermined levels of difference. Also shown is the Cohen's *d* trajectory comparing the eastern Boreal Shield trajectory means to the western Boreal Shield trajectory means

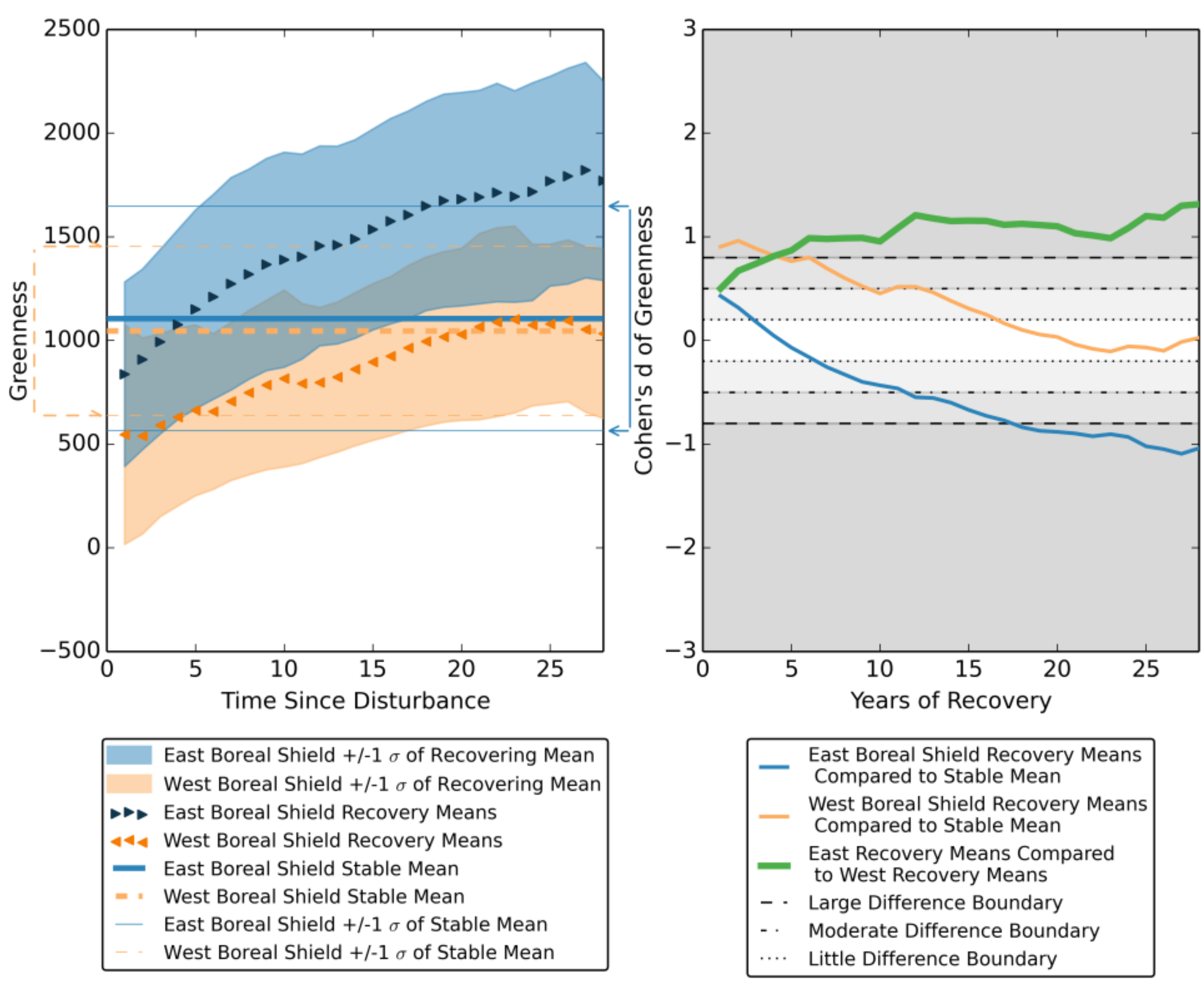

Figure 4: a) Observed Greenness recovery trajectory of each Boreal Shield section. Shading for each section shows +/-1 standard deviation of the recovery means per a year. Straight horizontal lines indicate the stable means and +/-1 standard deviation range for each Boreal Shield section. **b)** Cohen's *d* Greenness recovery trajectories for each Boreal Shield are shown with the predetermined levels of difference. Also shown is the Cohen's *d* trajectory comparing the eastern Boreal Shield trajectory means to the western Boreal Shield trajectory means

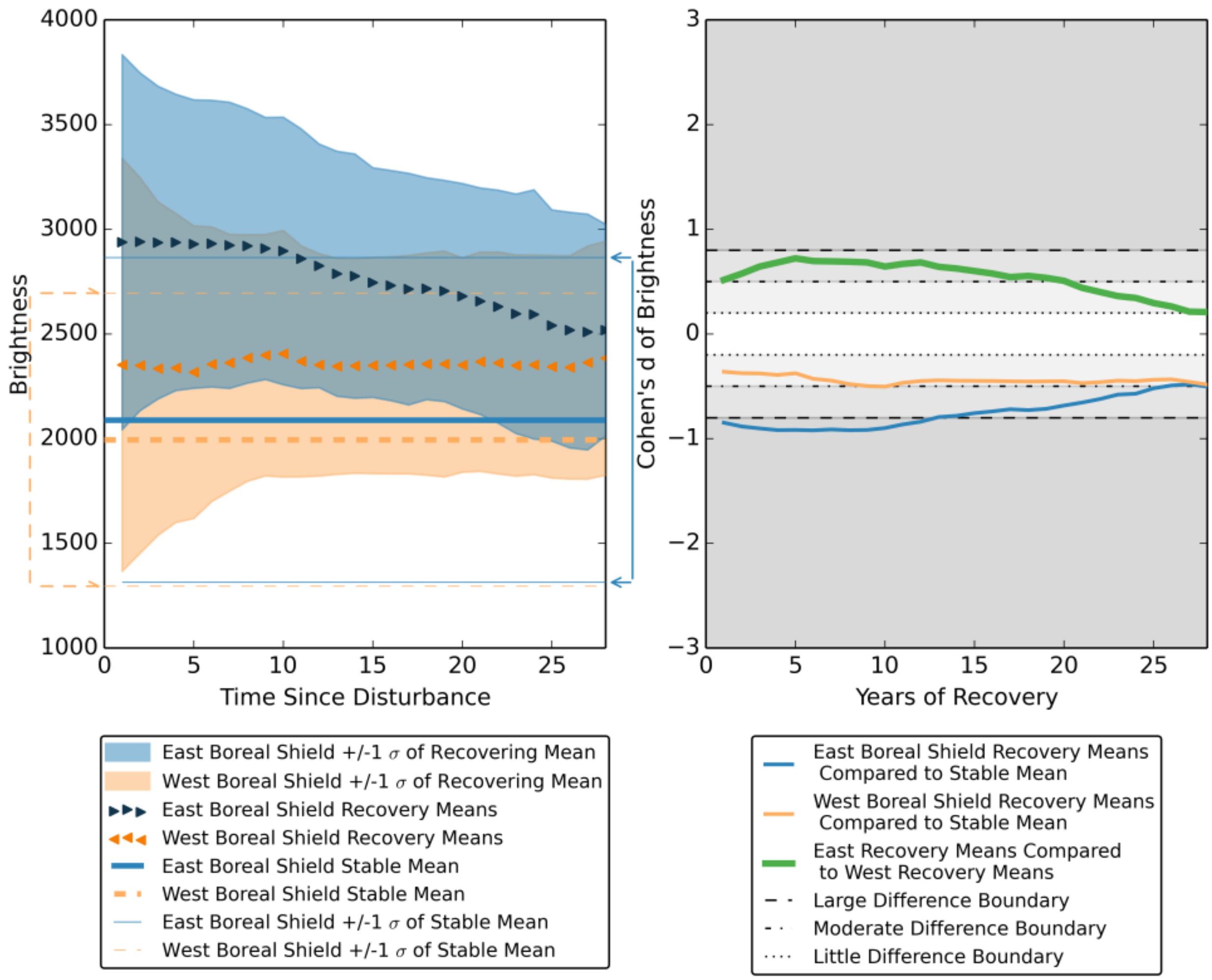

Figure 5: a) Observed Brightness recovery trajectory of each Boreal Shield section. Shading for each section shows +/-1 standard deviation of the recovery means per a year. Straight horizontal lines indicate the stable means and +/-1 standard deviation range for each Boreal Shield section. **b)** Cohen's *d* Brightness recovery trajectories for each Boreal Shield are shown with the predetermined levels of difference. Also shown is the Cohen's *d* trajectory comparing the eastern Boreal Shield trajectory means to the western Boreal Shield trajectory means.

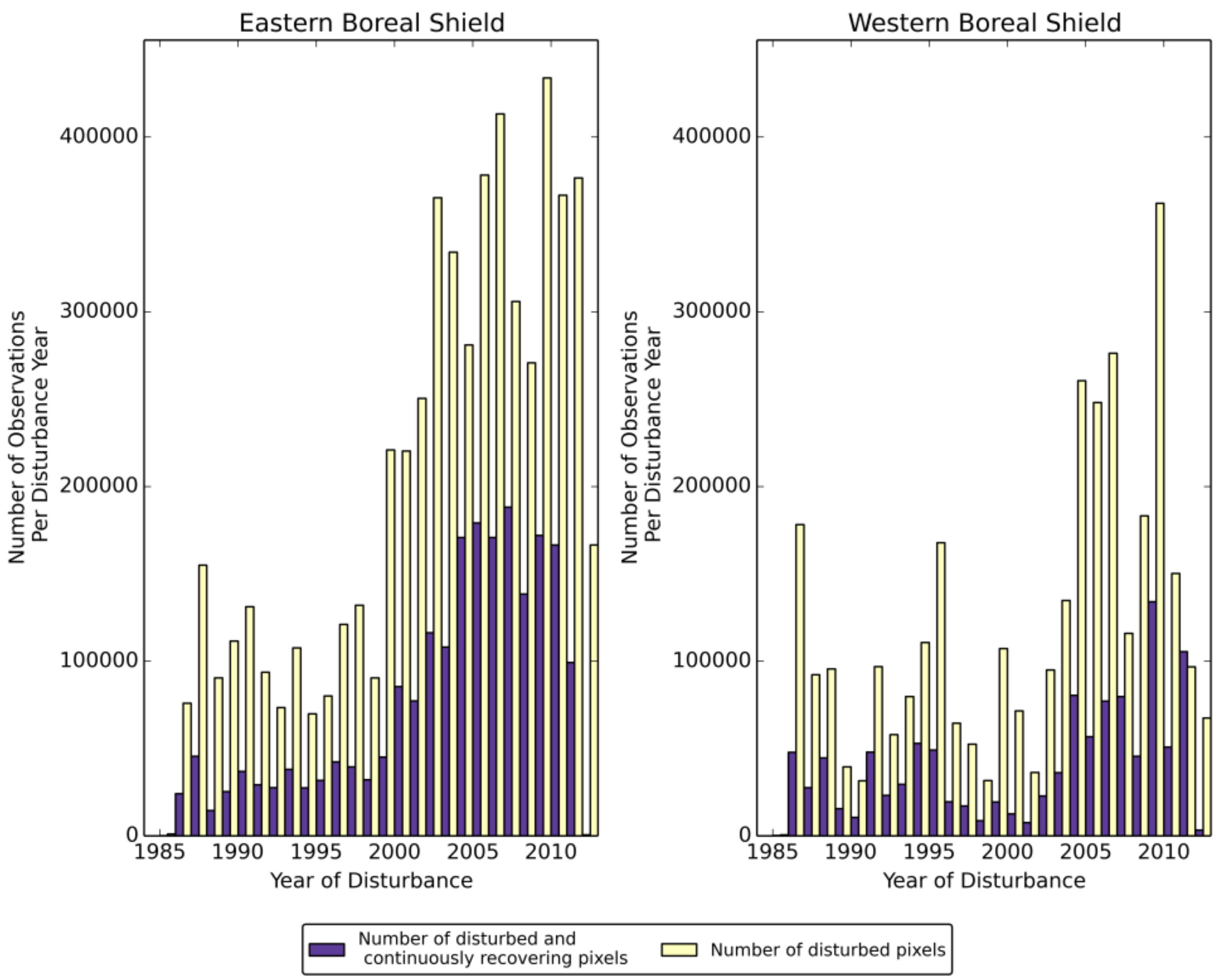

Figure 6: Number of disturbed pixels per year, and number of analysed pixels that were disturbed and recover unabatedly through the end of their time series for the **a)** eastern study areas and **b)** western study areas.

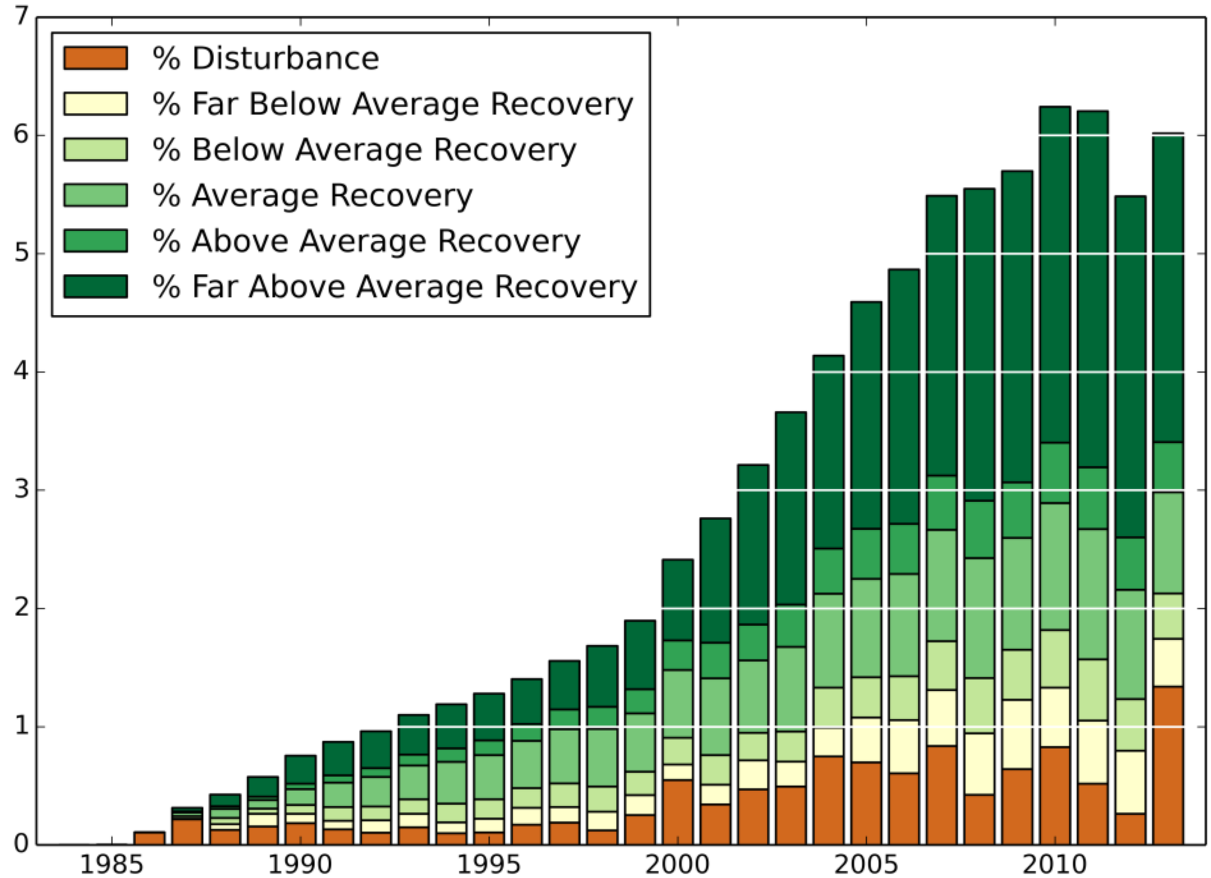

Figure 7: Boreal Shield East study areas spatial disturbance and recovery trends shown as a percent of the total forest area in the study areas. Disturbance is calculated annually. Recovery is cumulative and the categories of recovery are classified into five categories based on the recovery trajectory means and standard deviations from the Wetness trajectories in Figure 3a.

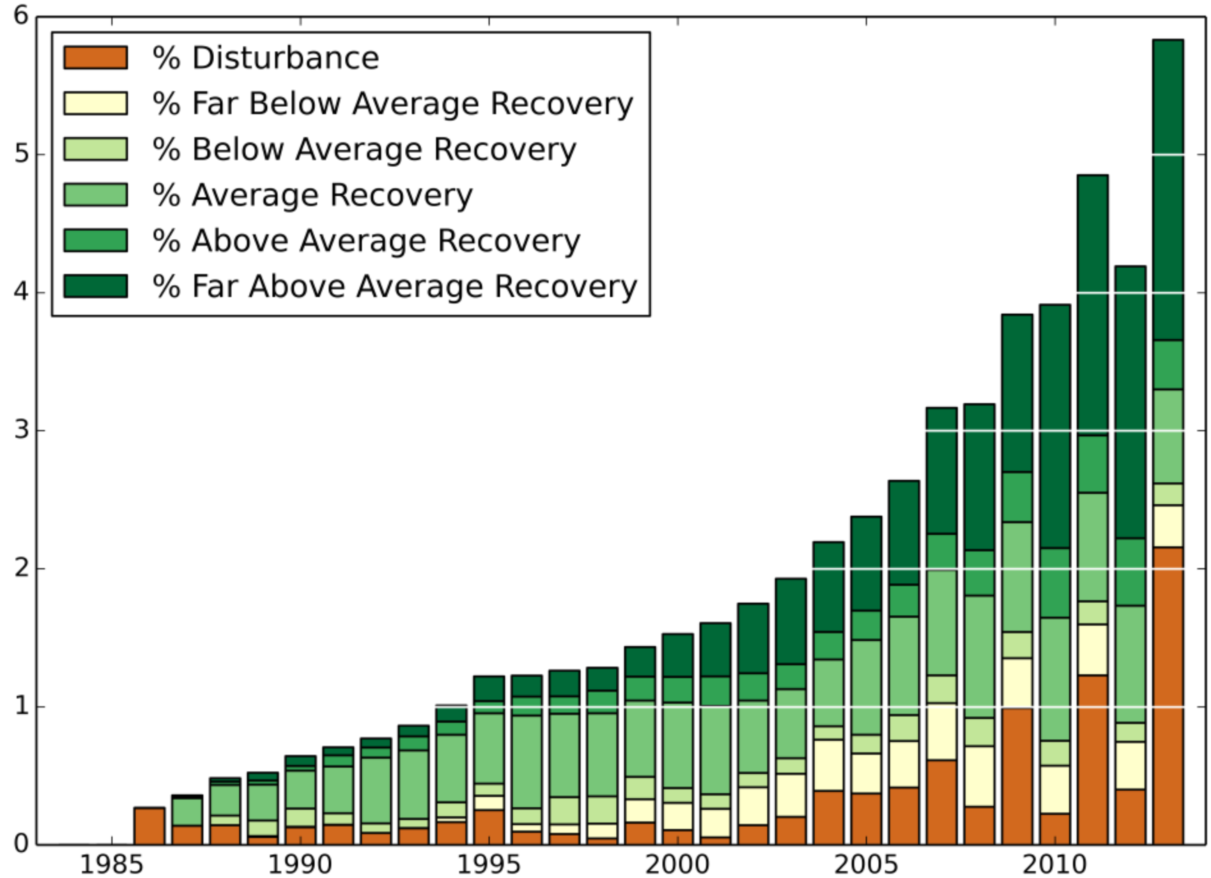

Figure 8: Boreal Shield West study areas spatial disturbance and recovery trends shown as a percent of the total forest area in the study areas. Disturbance is calculated annually. Recovery is cumulative and the categories of recovery are classified into five categories based on the recovery trajectory means and standard deviations from the Wetness trajectories in Figure 3a.

Tables

Table 1: Summary statistics about each Landsat scene's management and inventory area, showing the individual path rows from which scene portions were used to construct the Landsat time series and the amount of boreal forest present in each scene. The amount of area experiencing each type of management paradigm in each Boreal Shield section and as a percent of the total forested area in that Boreal Shield section and management zone is also displayed in Table 1. Table 1 additionally enumerates the total area under study per a Boreal Shield section and as a percent of the total forested area within that Boreal Shield section. The values reflected in Table 1 show that we have divided our study areas as evenly as possible between zones of management and Boreal Shield East and West sections.

Ecozone Name	Boreal Forest Managed/ Unmanaged	WRS2 Path and Row Portion	Boreal Forest Area in Scene (km^2)	Study Zone Area per Management (km^2)	Study Zone Area as a % of Ecozone per Management	Total Study Zone Area in Ecozone (KM^2)	Total Study Zone Area as a % of Ecozone
Boreal Shield East	Managed	17/26	31649	62592	7.60%	97865	11.89%
		12/25	30943				
	Unmanaged	13/23	11571	35272	4.29%		
		16/24	23701				
Boreal Shield West	Managed	31/21	15742	46078	5.88%	105485	13.47%
		27/24	30336				
	Unmanaged	26/23	29305	59406	7.58%		
		38/20	30101				

Table 2: Summarization of Cohen's *d* trajectories by difference category and values at the start, midpoint, and end of the trajectory for Brightness, Greenness, and Wetness comparing east and west Boreal Shield recovery means to their stable means, and comparing eastern Boreal Shield recovery means to western Boreal Shield recovery means.

	East Recovery Means vs East No Change Stable Forest Mean			West Recovery Means vs West No Change Stable Forest Mean			East to West Comparison of Recovery Means		
Recovery Year	1	14	28	1	14	28	1	14	28
Brightness	-0.84	-0.74	-0.49	-.036	-0.45	-0.48	0.51	0.62	0.21
Greenness	0.49	-0.60	-104	0.90	0.39	0.03	0.50	1.51	1.31
Wetness	2.09	0.98	0.02	1.31	0.97	0.37	0.01	0.61	0.90

Levels of Difference:	Large	Moderate	Little	None